

Pump modulation of a two-mode Fabry-Pérot laser: Influence of an internal resonance

D. Pieroux, T. Erneux, and Paul Mandel

Université Libre de Bruxelles, Optique Nonlinéaire Théorique, Campus Plaine, Code Postal 231, 1050 Bruxelles, Belgium

(Received 28 February 1996)

We study the response of a two-mode laser to an external periodic pump modulation of small amplitude. The control parameters are the pump-modulation frequency and amplitude. We first show that the ratio of the two relaxation oscillation frequencies may be commensurate. We then investigate the parameter domain in which the lowest of the two relaxation oscillation frequencies is close to half the other relaxation oscillation frequency. We derive analytically a pair of nonlinear amplitude equations for the dynamical modes of the system. This gives access to the stability of the time-periodic solutions that oscillate at the pump-modulation frequency and its first (sub)harmonic. It also determines the occurrence of secondary bifurcations leading to more complex solutions. [S1050-2947(96)08909-3]

PACS number(s): 42.55.-f, 42.65.Sf, 42.60.Mi

I. INTRODUCTION

The modal self-organization of multimode lasers is nowadays a field of active research. This is mainly due to the complex dynamics displayed by these systems and by the success of the theory to predict or explain the experimental results. In this context, there has recently been a renewed interest in the model proposed by Tang, Statz, and deMars (TSD) [1]. This model describes a N -mode free-running Fabry-Pérot solid-state laser for which atomic polarization can be adiabatically eliminated (rate equation approximation). Its main feature is that the effects of the population inversion grating caused by spatial hole burning are taken into account. Multimode lasers governed by the TSD equations display no oscillatory instabilities. Hence, in the long-time limit, they relax always to the single stable steady state. For each of the N modes, this relaxation occurs via damped oscillations characterized by N frequencies and $N+1$ damping rates. However, under conditions which are easily achieved for solid-state lasers, the total intensity (viz., the sum of the modal intensities) is characterized by only one frequency and one damping rate, as if it were a single mode laser. This frequency is the relaxation oscillation frequency or McCumber frequency [2] and corresponds to the largest of the N modal frequencies. The property that only one frequency is associated with the dynamics of the total intensity has been called antiphase dynamics (AD) in laser physics. This modal self-organization is a basic property found not only in the transient relaxation to the steady state, but also in the output of externally modulated and in chaotic lasers as well as in the noise spectrum of cw lasers [3–10]. In laser physics, AD has been found first in lasers with intracavity second-harmonic generation in the self-pulsing regime [11–16]. It was shown recently that this problem has unexpected links with the TSD equation [17]. An attempt to classify the different types of antiphased states has been undertaken in [18] and [19].

The N -mode TSD equations we shall consider [1] are given by

$$\begin{aligned}\frac{dN_0}{dt} &= w - N_0 - \sum_{k=1}^N \gamma_k (N_0 - N_k/2) I_k, \\ \frac{dN_m}{dt} &= \gamma_m N_0 I_m - N_m \left(1 + \sum_{k=1}^N \gamma_k I_k \right),\end{aligned}\quad (1)$$

$$\frac{dI_m}{dt} = \kappa I_m [\gamma_m (N_0 - N_m/2) - 1], \quad m = 1, 2, \dots, N.$$

In these equations, I_m is the intensity of the mode m . The space averaged population inversion N_0 and the population inversion gratings N_m are related to the population inversion $N(x, t)$ inside the cavity through

$$N_0 = \frac{1}{L} \int_0^L N(x, t) dx,$$

$$N_m = \frac{2}{L} \int_0^L N(x, t) \cos(2k_m x) dx,$$

where k_m is the wave number of mode m and L is the length of the cavity which is entirely filled by the active medium. The pump parameter w is normalized in such a way that the laser first threshold corresponds to $w=1$. The gain of mode m relative to the gain of mode 1 is $\gamma_m \leq 1$, and κ is the inverse photon lifetime in the cavity. As usual, all decay rates are assumed to be the same for each mode [1]. For solid-state lasers, κ is a large quantity being typically of order 10^4 to 10^6 . The dimensionless time t is measured in units of the population inversion relaxation time.

The analytical study of the TSD equations was initiated in [5]. In [7], a reference model was derived and analyzed by assuming $\gamma_m=1, \forall m$. Although this is a drastic simplification, many properties of the system are preserved. The reference model predicts two oscillation frequencies, namely, Ω_R and $\Omega_L < \Omega_R$. Owing to the mode equivalence, Ω_L is $(N-1)$ degenerate. In the general case (e.g., $\gamma_1=1, \gamma_m < 1$), Ω_L splits into $N-1$ different frequencies [7].

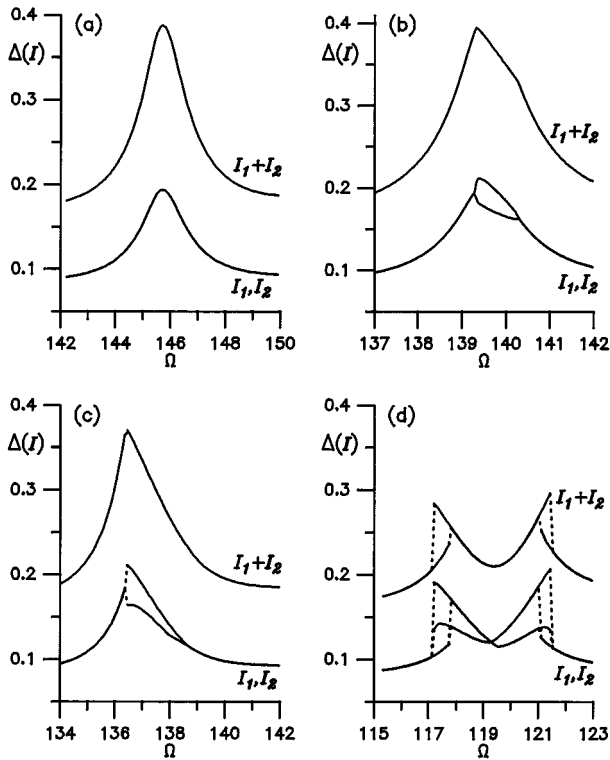


FIG. 1. Oscillation amplitude of I_1 , I_2 and I_1+I_2 . $\Delta(I)$ is defined as $\max_t[I(t)] - \min_t[I(t)]$ over the period of the oscillations. The average pump value is (a) 2.70, (b) 2.56, (c) 2.50, and (d) 15/7. The corresponding frequency ratios Ω_R/Ω_L are (a) 1.948, (b) 1.956, (c) 1.964, and (d) 2. The other parameters are $\gamma_1=\gamma_2=1$, $M=0.075$, and $\kappa=5\times 10^4$. The dotted lines represent jumps between two periodic solutions. A hysteresis is clearly observed in (d).

Another property of the reference model is that the ratio between the two frequencies Ω_R and Ω_L is bounded: $2N-1 \leq (\Omega_R/\Omega_L)^2 \leq 2N+1$. If $N=2$, the remarkable relation $\Omega_R/\Omega_L=2$ happens for the particular pump value $w_{\text{res}}=15/7$. In this case, since the two frequencies are commensurate, resonant couplings occur between them.

The purpose of this paper is to study, analytically, such resonant couplings in the vicinity of $\Omega_R/\Omega_L \approx 2$. This is achieved by probing the laser with a small amplitude pump modulation whose frequency Ω_{ext} is close to either Ω_L or Ω_R . In Fig. 1, the effects of the resonant coupling can be observed. In this figure, the two modes have been chosen equivalent, i.e., $\gamma_1=\gamma_2=1$. The oscillation amplitude Δ of I_1 , I_2 , and I_1+I_2 are plotted as functions of the pump-modulation frequency, chosen in the neighborhood of Ω_L . The pump-modulation amplitude is $M=0.075$. By progressively decreasing the average pump value, the ratio Ω_R/Ω_L increases from Fig. 1(a) to 1(d). In Fig. 1(a), $\Omega_R/\Omega_L=1.948$ and a single peak is observed. This peak is shifted towards the low frequencies relative to the value obtained by the linear approximation [$\Omega_L(\text{linear})=149.7$]. In Fig. 1(b), $\Omega_R/\Omega_L=1.959$ and a symmetry breaking appears between I_1 and I_2 , leading to bistable states. For $\Omega_R/\Omega_L=1.964$ [Fig. 1(c)], a discontinuity is clearly observed in the curves. More precisely, this discontinuity results from a hysteresis, whose range is too thin to be noticed on the figure. By increasing Ω_R/Ω_L towards two, a second hysteresis phenomenon ap-

pears on the right side of the peak. The fully developed case is shown in Fig. 1(d) for $\Omega_R/\Omega_L=2$. Moreover, AD is clearly present in Fig. 1(d) since $\Delta(I_1)+\Delta(I_2) \geq \Delta(I_1+I_2)$, which is not the case in Figs. 1(a)–(c).

Of particular physical interest is how AD depends on the resonant interactions between modes and on the modulation frequency Ω_{ext} . As will be demonstrated, a strong selection between temporal patterns results from the modulation of the two-mode laser. A general observation of our analysis is that the simplest model we developed already captures the condition for pure AD, pure in-phase regimes and mixed anti- and in-phase regimes.

When a nonlinear system is subject to a periodic modulation, the natural tool to analyze its response is the power spectrum. Unless the dynamics is chaotic, each oscillation frequency present in the system appears as a peak. The peak position indicates the frequency and its height measures the amplitude of the oscillation at that frequency. General relations between the power spectra of the modal intensities and of the total intensity at Ω_L and Ω_R have recently been found theoretically and experimentally [20,21]. In this paper, we extend these results by computing the height of these peaks as a function of the pump-modulation amplitude.

In Sec. II, relations existing between the frequencies of a N -mode laser are derived. The simple case of a two-mode laser is also treated with more details. The analytical model describing the modulated two-mode laser dynamics is the object of Sec. III. The simplest case, called the reference model with modulation, is then studied in detail in Sec. IV, while other cases leading to secondary bifurcations are investigated in Sec. V. In Sec. VI the validity of our analytical results is discussed by comparing them with numerical simulations. Finally, we conclude in Sec. VII.

II. FREQUENCY PROPERTIES

Many nonlinear dynamical systems described by ordinary differential equations admit steady-state solutions, i.e., solutions that do not involve time. If such a steady state is slightly perturbed, the system relaxes either back to or away from it. The usual method to study the stability of a steady-state solution is to examine the roots λ of the characteristic polynomial. The real part of each λ is a measure of the rate at which the system relaxes to or away from the steady state, depending on whether $\text{Re}(\lambda) < 0$ or $\text{Re}(\lambda) > 0$, respectively. The imaginary part of λ , if any, corresponds to a relaxation frequency. For the N -mode TSD equations, the degree of the characteristic polynomial is $2N+1$. This means it cannot be solved exactly for arbitrary N . However, most free-running solid-state lasers modeled by the TSD equations exhibit $\kappa \gg 1$, suggesting an asymptotic approximation. In [7], it was shown how to exploit the limit $\kappa \gg 1$ by rewriting Eqs. (1) in terms of the deviations from the stable steady state. To this end, we introduce the small parameter $\delta=1/\sqrt{\kappa}$ and the variables σ , n_0 , n_m , and s_m defined by

$$\sigma \equiv t/\delta,$$

$$n_0 \equiv (N_0 - N_0^0)/\delta, \quad n_m \equiv (N_m - N_m^0)/\delta \quad (3)$$

$$s_m \equiv I_m - I_m^0,$$

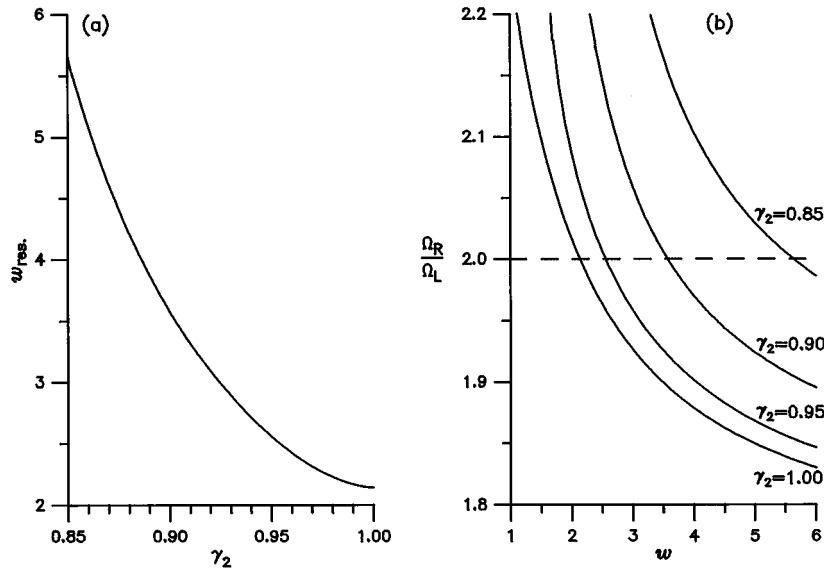


FIG. 2. Resonance between the two relaxation frequencies Ω_L and Ω_R . (a) $w_{\text{res}}(\gamma_2)$ at which $\Omega_R/\Omega_L=2$ based on the analytical expression (11). (b) Numerical computation of Ω_R/Ω_L for a range of w and γ_2 .

where the superscript 0 indicates the steady-state solution given by

$$w = N_0^0 + \frac{N_0^0 S_1 - S_2}{S_1 - \left(N - \frac{1}{2}\right) N_0^0},$$

$$N_m^0 = 2(N_0^0 - 1/\gamma_m), \quad I_m^0 = \frac{1}{\gamma_m} \frac{N_0^0 - 1/\gamma_m}{S_1 - \left(N - \frac{1}{2}\right) N_0^0} \quad (4)$$

$$\text{with } S_1 \equiv \sum_{k=1}^N \frac{1}{\gamma_k}, \quad S_2 \equiv \sum_{k=1}^N \frac{1}{\gamma_k^2}.$$

After inserting Eqs. (3) into Eqs. (1), the limit $\delta \rightarrow 0$ is taken. The resulting equations are then linearized and reduced to

$$\frac{dn_0}{d\sigma} = - \sum_k s_k,$$

$$\frac{dn_m}{d\sigma} = \gamma_m s_m N_0^0 - N_m^0 \sum_k \gamma_k s_k, \quad (5)$$

$$\frac{ds_m}{d\sigma} = \gamma_m I_m^0 (n_0 - n_m/2).$$

To proceed analytically with the N -mode case, we restrict the analysis to the degenerated case $\gamma_m = 1, \forall m$. As a result, all the modal intensities are equal, i.e., $I_m^0 = \mathcal{I}, \forall m$. The eigenvalues of system (5) can then be computed analytically. They are 0, $\pm\Omega_L$, $\pm\Omega_R$ with $\Omega_L = (\mathcal{I}N_0^0/2)^{1/2}$ and $\Omega_R = (\mathcal{I}N + N_0^0 - 1)^{1/2}$ [7]. By using Eqs. (4), we note that

$$\frac{\Omega_R^2}{\Omega_L^2} = 1 - 2N + \frac{4N}{N_0^0}. \quad (6)$$

Letting N_0 vary from 1 at $w=1$ (laser first threshold) to $N_0 = N/(N-1/2)$ at $w=\infty$, the lower and upper bounds for Ω_R^2/Ω_L^2 are obtained from Eq. (6).

$$2N - 1 \leq \frac{\Omega_R^2}{\Omega_L^2} \leq 2N + 1. \quad (7)$$

If the ratio Ω_R/Ω_L is rational, resonant interactions between the oscillations at Ω_R and Ω_L appear. Because of the quadratic nature of the nonlinearities of the TSD system (1), the simplest case $\Omega_R/\Omega_L \approx 2$ is expected to lead to strong resonant parametric interactions. As indicated by Eq. (7), this is possible only for $N=2$. In this case, it is found from Eqs. (4) and (6) that the exact resonance $\Omega_R/\Omega_L=2$ occurs for a pump value $w = w_{\text{res}} = 15/7$.

This result can be generalized to the asymmetric two-mode case $\gamma_1=1, \gamma_2<1$. Let us determine, for this general two-mode case, the pump value under which exact resonance happens. The characteristic polynomial of Eqs. (5) factors out into $\lambda P_2(\lambda^2)$ where the biquadratic polynomial $P_2(\lambda^2)$ is

$$P_2(\lambda^2) = 4\lambda^4 + 2\lambda^2[(4 - N_0^0)I_1^0 + \gamma_2(4 - \gamma_2 N_0^0)I_2^0] + \{\gamma_2[8 + 4(1 + \gamma_2)N_0^0 - 3\gamma_2(N_0^0)^2] - 4(1 + \gamma_2^2)\}I_1^0 I_2^0. \quad (8)$$

The imaginary part of the roots of $P_2(\lambda^2)$ gives two oscillating frequencies

$$\Omega_L = \frac{\sqrt{A - \sqrt{B}}}{2} \quad \text{and} \quad \Omega_R = \frac{\sqrt{A + \sqrt{B}}}{2}, \quad (9)$$

with

$$A = I_1^0(4 - N_0^0) + \gamma_2 I_2^0(4 - \gamma_2 N_0^0),$$

$$B = A^2 + 2I_1^0 I_2^0 \{2\gamma_2 N_0^0 [3\gamma_2 N_0^0 - 4(1 + \gamma_2)] + 8(1 - \gamma_2)^2\}. \quad (10)$$

The exact resonance condition $\Omega_R/\Omega_L=2$ requires

$$25B = 9A^2. \quad (11)$$

As A and B depend on w and γ_2 , Eq. (11) is a fourth degree polynomial in each of these two parameters. In Fig. 2(a), the implicit equation $25B = 9A^2$ has been solved numerically to obtain $w_{\text{res}}(\gamma_2)$. In Fig. 2(b), it is demonstrated that Ω_R/Ω_L remains in the vicinity of two over a large neighborhood of w around w_{res} . This explains why strong interactions between the two oscillating modes are observed even for w away from w_{res} , as is the case in Figs. 1(b) and 1(c).

III. AMPLITUDE EQUATIONS

In this section, we derive the amplitude equations of a weakly pump modulated two-mode TSD laser for which $w \approx w_{\text{res}}$ (i.e., for which $\Omega_R/\Omega_L \approx 2$). A perturbation method is used to take advantage of $\kappa \gg 1$. For the laser with modulation, it is mathematically more convenient to introduce a new small parameter

$$\epsilon \equiv \left(\frac{7}{2\kappa} \right)^{1/2}, \quad (12)$$

instead of δ . We then seek a solution of Eqs. (1) of the form

$$N_0(t) = N_0^0 + \epsilon^2 n_{0,1}(t) + O(\epsilon^2),$$

$$N_m(t) = N_m^0 + \epsilon^4 n_{m,1}(t) + O(\epsilon^2), \quad (13)$$

$$I_m(t) = I_m^0 + \frac{1}{2} s_{m,1}(t) + O(\epsilon), \quad m = 1, 2.$$

The problem is further restricted by considering γ_2 close to 1

$$\gamma_1 = 1, \quad \gamma_2 = 1 - \epsilon g + O(\epsilon^2). \quad (14)$$

In the unmodulated case [7], the results of this expansion hold for γ_2 as small as 0.8. However, an essential assumption for the derivation of the amplitude equations is that the dynamical variables N_0 , N_m , and I_m be explicit analytic functions of ϵ .

The pump is weakly modulated around $w_{\text{res}} = 15/7$ at an external frequency Ω_{ext} . This is expressed by

$$w(\epsilon) = \overline{w} + M(\epsilon) \cos(\Omega_{\text{ext}} t), \quad (15)$$

where

$$\overline{w} = \frac{15}{7} + \epsilon w_1 + O(\epsilon^2),$$

$$M = \epsilon^2 [M_1 + \epsilon M_2 + O(\epsilon^2)],$$

and w , M_1 , M_2 are parameters.

The external frequency is tuned to a value close to either Ω_L or Ω_R . This motivates the introduction of the basic time τ defined by

$$\tau \equiv \Omega_e t, \quad \text{where}$$

$$\Omega_e \equiv \frac{\Omega_{\text{ext}}}{\alpha} = \frac{1 + \epsilon \omega_e + O(\epsilon^2)}{\epsilon}, \quad (16)$$

with either $\alpha = 1$ if $\Omega_{\text{ext}} \approx \Omega_L$ or $\alpha = 2$ if $\Omega_{\text{ext}} \approx \Omega_R$. The aim of using α is to derive simultaneously the equations for

$\Omega_{\text{ext}} \approx \Omega_L$ and $\Omega_{\text{ext}} \approx \Omega_R$. By the way it is defined, Ω_e is always close to Ω_L . The detuning between Ω_L and Ω_e is measured by ω_e . Note that $\Omega_L = 1$ and $\Omega_R = 2$ with the scaling (16) for t if $\epsilon = 0$.

Introducing Eqs. (12) to (16) into Eqs. (1) and equating to zero the coefficients of ϵ^n gives a sequence of linear problems. To first order, the evolution equations are

$$\frac{dn_{0,1}}{d\tau} = -\frac{7}{4}(s_{1,1} + s_{2,1}) + M_1 \cos(\alpha\tau),$$

$$\frac{dn_{1,1}}{d\tau} = (3s_{1,1} - s_{2,1})/4,$$

$$\frac{dn_{2,1}}{d\tau} = (3s_{2,1} - s_{1,1})/4, \quad (17)$$

$$\frac{ds_{1,1}}{d\tau} = n_{0,1} - n_{1,1},$$

$$\frac{ds_{2,1}}{d\tau} = n_{0,1} - n_{2,1}.$$

The general solution of the linear system (17) is the solution of the homogeneous problem plus a particular solution. Let us write Eqs. (17) in compact form $d\vec{v}_1/d\tau = L\vec{v}_1 + N_1$ where $L\vec{v}_1$ and N_1 are, respectively, the homogeneous and the inhomogeneous parts of the right-hand side (rhs) of Eqs. (17). The general solution of the homogeneous problem $d\vec{v}_H/d\tau = L\vec{v}_H$ is

$$\vec{v}_H(\tau) = \vec{v}_0 e^{\lambda_0 \tau} + \sum_{i=L,R} [\vec{v}_i e^{\lambda_i \tau} + \text{c.c.}]. \quad (18)$$

In these equations, the λ 's and the \vec{v} 's (as well as their complex conjugates) are the eigenvalues and the eigenvectors of the matrix L

$$\lambda_0 = 0, \quad \vec{v}_0 \propto (1, 1, 1, 0, 0),$$

$$\lambda_L = i, \quad \vec{v}_L \propto (0, -i, i, 1, -1), \quad (19)$$

$$\lambda_R = 2i, \quad \vec{v}_R \propto (7i/4, -i/4, -i/4, 1, 1).$$

The oscillation amplitude of the total intensity is given, for each frequency, by the sum of the eigenvector's last two terms. This sum vanishes for \vec{v}_L but not for \vec{v}_R . Therefore, the low frequency Ω_L does not contribute to the total intensity, which oscillates only at Ω_R . This phenomenon is the signature of AD.

The inhomogeneous term \vec{N}_1 is $[M_1 \cos(\alpha\tau), 0, 0, 0, 0]$. If $\alpha = 2$, \vec{N}_1 oscillates at the resonant frequency $\Omega_R = 2$. Such a resonance with the homogeneous system leads to secular terms and unbounded solutions appear. The only way to avoid the divergence is to impose $M_1 = 0$. This constraints the pump oscillation amplitude to be an $O(\epsilon^2)$ quantity. If $\alpha = 1$, \vec{N}_1 oscillates at the resonant frequency $\Omega_L = 1$, but in this case \vec{N}_1 is orthogonal to \vec{v}_L . Because of this orthogonality, the secular divergence is avoided and the pump oscillation

tion amplitude can remain an $O(\epsilon)$ quantity. Also, the laser is much more sensitive to a modulation around Ω_R than around Ω_L , since the value of the pump modulation amplitude M required to produce similar laser intensity oscillation amplitudes is of order $1/\epsilon$ greater at Ω_L than at Ω_R . This is a well-known experimental property [4,22]. A similar result has been derived for pump-modulated multimode intracavity second harmonic generation (ISHG) lasers [23]. It is then easy to verify by direct substitution that $\vec{v} = (i, -i, -i, 2, 2)(M_1/12)e^{i\tau} + \text{c.c.}$ is a particular solution of Eqs. (17). Eventually, the general solution of Eqs.(17) reads

$$\begin{pmatrix} n_{0,1} \\ n_{1,1} \\ n_{2,1} \\ s_{1,1} \\ s_{2,1} \end{pmatrix} = 2ia \begin{pmatrix} 7i/4 \\ -i/4 \\ -i/4 \\ 1 \\ 1 \end{pmatrix} e^{2i\tau} + \begin{pmatrix} iP_\alpha/12 \\ i(-2ib - P_\alpha/12) \\ i(2ib - P_\alpha/12) \\ 2ib + P_\alpha/6 \\ -2ib + P_\alpha/6 \end{pmatrix} e^{i\tau} + c \begin{pmatrix} 1 \\ 1 \\ 1 \\ 0 \\ 0 \end{pmatrix} + \text{c.c.}, \quad (20)$$

where $P_{\alpha=1} \equiv M_1$, $P_{\alpha=2} \equiv 0$ and a, b, c are unknown amplitudes. It is worth noting that a is the amplitude of an in-phase oscillation around Ω_R , P_α that of an in-phase oscillation around Ω_L , and b that of an antiphase oscillation around Ω_L . Thus, it is already clear from the first-order solution (20) that in case of a modulation at $\Omega_{\text{ext}} \approx \Omega_R$, as P_2 is null, there is no in-phase modulation around Ω_L .

The $O(\epsilon^2)$ problem has to be considered in order to determine a, b , and c . This problem differs from Eqs.(17) only by the inhomogeneous term: $d\vec{v}_2/d\tau = L\vec{v}_2 + \vec{N}_2$ (\vec{N}_2 is given in the Appendix). It leads to secular terms and thus unbounded solutions. To avoid this unphysical situation, a, b , and c are assumed to depend on a slow time $\eta \equiv \epsilon\tau$. In this way, a multiple time-scale analysis is undertaken. Because τ and η have to be treated as two independent variables, the chain rule $d/d\tau = \partial/\partial\tau + \epsilon\partial/\partial\eta$ applies. Doing that, cancellation of the secular terms requires a, b , and c to satisfy three compatibility equations. One of these compatibility equations is

$$\frac{dc}{d\eta} = -\frac{53}{32}c. \quad (21)$$

Obviously, c decays exponentially to zero. Therefore, it can be neglected as we are not interested by the transient behavior of the laser. The two other compatibility equations are

$$\begin{aligned} \frac{da}{d\eta} &= -i\omega_2 a - \frac{75}{64}a - b^2 + m_\alpha, \\ \frac{db}{d\eta} &= -i\omega_1 b - b + ab^* + l_\alpha, \end{aligned} \quad (22)$$

where the coefficients are defined by

$$\omega_1 \equiv \omega_e + \frac{225}{424}g - \frac{105}{212}w_1,$$

$$\omega_2 \equiv 2\omega_e + \frac{15}{16}g - \frac{7}{8}w_1,$$

$$l_\alpha \equiv \frac{3g}{32}P_\alpha,$$

$$m_{\alpha=1} \equiv \frac{1}{144}M_1^2, \quad m_{\alpha=2} \equiv -\frac{1}{16}M_2. \quad (23)$$

Equations (22) are the amplitude equations of the laser oscillations. They describe the slow time dynamics of the weakly modulated laser. The analysis of these equations will be the main purpose of the next two sections.

Equations (22) are formally equivalent to the equations used to describe nonequilibrium phase transitions in subsecond-harmonic generation [24,25]. In that context, a nonlinear crystal is placed inside an optical cavity. An external coherent pumping field is used to maintain the system in a nonequilibrium state. The crystal transfers energy between two optical modes of the cavity via two photons processes. If the ratio of the two optical frequencies is close to two, either second-harmonic generation (SHG) or degenerated optical parametric oscillations (DOPO) appear, depending on the pumping field frequency. These systems also exhibit squeezing properties [26,27]. Because of this formal link, results well known for SHG or DOPO systems can be formally translated for the two-mode pump-modulated laser.

To conclude with this section, let us consider the physical meaning of the parameters appearing in Eqs. (22). The driving terms m and l are related to the pump-modulation amplitude M , while ω_1 (resp. ω_2) is the detuning between Ω_L and Ω_e (resp. Ω_R and $2\Omega_e$) at order ϵ . In the absence of external modulation, i.e., if $M=0=l=m$, it can be shown that $d(|a|^2 + |b|^2)/d\eta \leq 0$. By this we mean that the system always relaxes to its trivial solution $a=b=0$. This result eliminates the possibility of having isolated solutions.

IV. THE REFERENCE PROBLEM WITH MODULATION

Equations (22) are first investigated by considering the simplest case, namely, $g=w_1=\omega_1=\omega_2=l=0$. In terms of the initial parameters, that corresponds to $\gamma_2=1$, $\bar{w}=w_{\text{res}}=15/7$ and Ω_{ext} equals to either Ω_L or Ω_R . This will serve as the reference problem. Under these assumptions Eqs. (22) reduce to the tuned DOPO equations

$$\frac{da}{d\eta} = -\frac{75}{64}a - b^2 + m_\alpha, \quad (24)$$

$$\frac{db}{d\eta} = -b + ab^*.$$

These equations have already been widely studied [24,25]. They admit two steady-state solutions

$$\begin{aligned} a &= \frac{64}{75}m_\alpha, \quad b=0, \quad \text{which is stable for} \\ 0 &\leq m_\alpha \leq m_{\text{thr}} = \frac{75}{64}, \end{aligned} \quad (25)$$

and

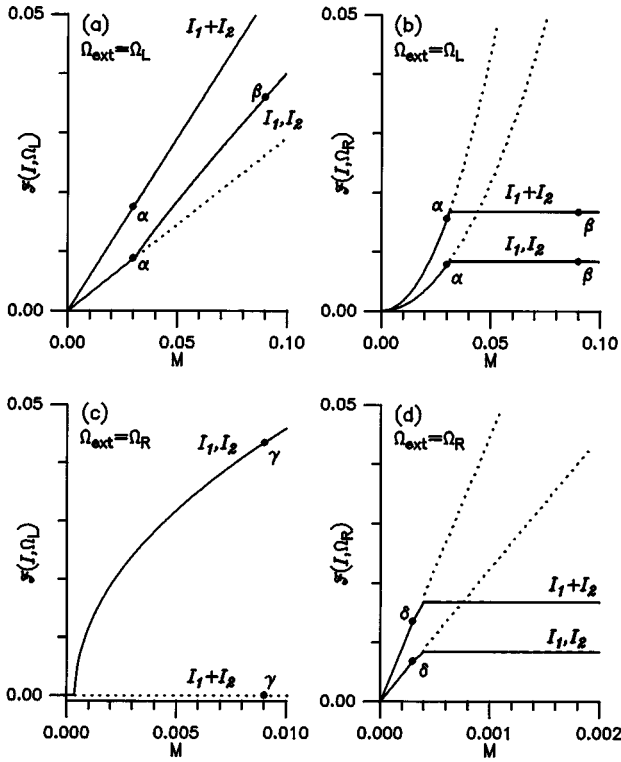


FIG. 3. Reference problem with modulation: analytical results. (a) and (c): Ω_L peak height of the Fourier spectra of I_1 , I_2 and $I_1 + I_2$. The pump-modulation frequency Ω_{ext} is (a) Ω_L and (c) Ω_R . (b) and (d): same as (a) and (c) for the Ω_R Fourier peak height. The points α , β , γ , and δ correspond to typical dynamical behaviors that are illustrated in Fig. 4. Stable solutions are plotted in full lines, unstable ones in dotted lines. The other parameters are $\kappa = 510^4$, $\bar{w} = 15/7$, $\gamma_1 = \gamma_2 = 1$.

$$a = 1, \quad b^2 = m_\alpha - \frac{75}{64}, \quad \text{which is stable for } m_{\text{thr}} \leq m_\alpha. \quad (26)$$

In Fig. 3, the laser behavior is analyzed in terms of the Fourier peak heights $\mathcal{F}(I, \Omega)$ with $I = I_1, I_2$ or $I_1 + I_2$. In this expression, Ω is the frequency of the peak studied. $\mathcal{F}(I, \Omega)$ is defined by

$$\mathcal{F}(I, \Omega) \equiv \left| \frac{\Omega_L}{2\pi} \int_0^{2\pi/\Omega_L} I(t) e^{i\Omega t} dt \right|. \quad (27)$$

The function $\mathcal{F}(I, \Omega)$ is computed from Eqs. (13), (20), and either (25) or (26) in order to get $I(t)$. The upper bound of the integration in the definition (27) corresponds to the period of the modal intensities I_1 and I_2 (taking into account the fact that a period doubling could happen for a modulation at Ω_R). As can be observed in Fig. 3, $\mathcal{F}(I_1, \Omega_{R,L})$ equals $\mathcal{F}(I_2, \Omega_{R,L})$ whether Ω_{ext} equals Ω_L or Ω_R . This equality holds because the terms $2ib + P_\alpha 16$ and $-2ib + P_\alpha 16$ of the linear solution (20) have the same modulus (b and P_α being real in the reference problem). They thus give the same peak height. The triangular inequality leads to

$$\mathcal{F}(I_1 + I_2, \Omega_L) \leq \mathcal{F}(I_1, \Omega_L) + \mathcal{F}(I_2, \Omega_L), \quad (28)$$

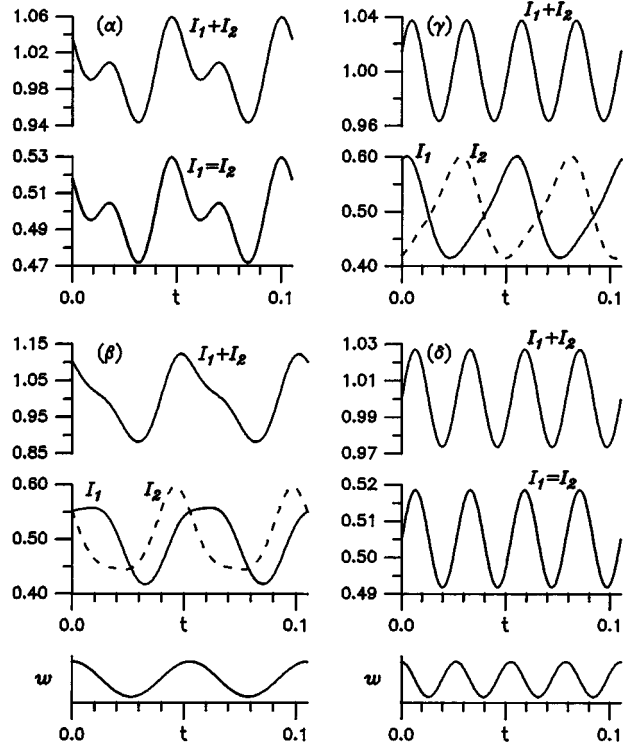


FIG. 4. Time evolution of $I_1(t)$, $I_2(t)$ and $I_1(t) + I_2(t)$ illustrating typical dynamical behaviors of the modulated laser. Each plot corresponds to a point indicated in Fig. 3: α ($M = 0.03$), β ($M = 0.09$), γ ($M = 0.009$), and δ ($M = 0.0003$). The other parameters are the same as in Fig. 3. I_1 and I_2 are represented by full and dotted lines, respectively, when they are not equal (i.e., when AD is present). On the bottom, $w(t)$ has been plotted to give a phase reference.

where the equality is satisfied if there is no antiphased oscillation, i.e., if $m_\alpha < m_{\text{thr}}$. On the other hand, since there is no antiphased oscillation at Ω_R , we have

$$\mathcal{F}(I_1 + I_2, \Omega_R) = \mathcal{F}(I_1, \Omega_R) + \mathcal{F}(I_2, \Omega_R). \quad (29)$$

The time evolution of I_1 , I_2 and $I_1 + I_2$ is displayed in Fig. 4 for four characteristic points labeled α , β , γ and δ in Fig. 3. The points α and δ correspond to $m_\alpha < m_{\text{thr}}$, implying $b = 0$ and thus no antiphased behavior. The presence of AD is revealed by the difference existing between I_1 and I_2 , as shown for the points β and γ , for which $m_\alpha > m_{\text{thr}}$. A spectacular effect of AD occurs around the point γ : each modal intensity I_1 and I_2 strongly oscillates at Ω_L while their sum $I_1 + I_2$ oscillates only at Ω_R . This comes from the fact that the external modulation being at Ω_R , the in-phase Ω_L oscillation term P_2 cancels identically [see solution (20)], while the antiphase Ω_L oscillation found in I_1 and I_2 interferes destructively in $I_1 + I_2$. There is thus no trace of the Ω_L oscillation in the total intensity.

V. THE GENERAL CASE

The full system Eqs. (22) is now investigated. The detunings ω_1 and ω_2 do not cancel either if the exact resonant condition $\Omega_R = 2\Omega_L$ is not satisfied [i.e., if $w \neq w_{\text{res}}(\gamma_2)$], or

if the external frequency Ω_{ext} is not exactly tuned to Ω_L or Ω_R .

However, there are two cases for which the driving amplitude l_α cancels. First, l_α cancels if the external modulation frequency Ω_{ext} is close to Ω_R . Second, l_α cancels if $\gamma_2=1$, whatever the external modulation frequency is. Then, Eqs. (22) reduce to the equations for the DOPO with detuning [24,25]. These equations admit two steady-state solutions which are more easily described by the new complex variable $X=b^2$. From Eqs. (22), an equation for X is derived

$$\left[\left(\frac{75}{64} - \omega_1\omega_2 + |X|\right) + i\left(\frac{75}{64}\omega_1 + \omega_2\right)\right]X = m_\alpha |X|. \quad (30)$$

This equation admits a trivial solution $X_0=0$. In terms of the amplitudes a and b , it corresponds to

$$a = \frac{m_\alpha}{(75/64) + i\omega_2}, \quad b = 0. \quad (31)$$

The trivial solution is stable for $0 \leq m_\alpha \leq m_{\text{thr}} = [|(1+i\omega_1)(75/64+i\omega_2)|]^{1/2}$.

To find the nontrivial solutions of Eq. (30), the equation is multiplied by its complex conjugate. This yields a quadratic equation in $|X|$ whose solutions are

$$|X_\pm| = -\frac{75}{64} + \omega_1\omega_2 \pm [m_\alpha^2 - (\frac{75}{64}\omega_1 + \omega_2)^2]^{1/2}. \quad (32)$$

As $|X_\pm|$ must be real and positive, there are restrictions on the scaled-modulation amplitude m_α . Depending on ω_1 and ω_2 , two possibilities exist. If $\omega_1\omega_2 \leq 75/64$, $|X_+|$ exists for $m_\alpha \geq m_{\text{thr}}$ and bifurcates from X_0 at $m_\alpha = m_{\text{thr}}$, while $|X_-|$ does not exist. On the other hand, if $\omega_1\omega_2 > 75/64$, both $|X_+|$ and $|X_-|$ exist within a given range of m_α . The domain of existence of $|X_+|$ is $m_\alpha \geq m_{\text{lim}} = |(75/64)\omega_1 + \omega_2|$. The domain of existence of $|X_-|$ is $m_{\text{lim}} \leq m_\alpha \leq m_{\text{thr}}$. $|X_-|$ bifurcates from X_0 at m_{thr} and joins $|X_+|$ at the limit point m_{lim} . Over the domain of existence of $|X_-|$, bistability occurs between the trivial solution X_0 and $|X_+|$, since $|X_-|$ is always unstable.

In order to study the bistable regime, a and b have to be solved as functions of m_α , and this requires the determination of X . From Eqs. (30) and (32) the real and the imaginary parts of X are found to be

$$\begin{aligned} \text{Re}(X_\pm) &= \pm |X_\pm| \frac{[m_\alpha^2 - (\frac{75}{64}\omega_1 + \omega_2)^2]^{1/2}}{m_\alpha}, \\ \text{Im}(X_\pm) &= -|X_\pm| \frac{\frac{75}{64}\omega_1 + \omega_2}{m_\alpha}. \end{aligned} \quad (33)$$

Finally, a and b are given by

$$a_\pm = (1+i\omega_1) \frac{X_\pm}{|X_\pm|}, \quad b_\pm^2 = X_\pm. \quad (34)$$

The solution (34) shows that, for the nontrivial solution, the modulus of a is constant as it was in the reference problem with modulation. However, its phase is now a function of m_α .

Solution (34) leads to an indetermination of π on the phase of b . This indetermination finds its origin in the amplitude equations (22) which are invariant for a change of b

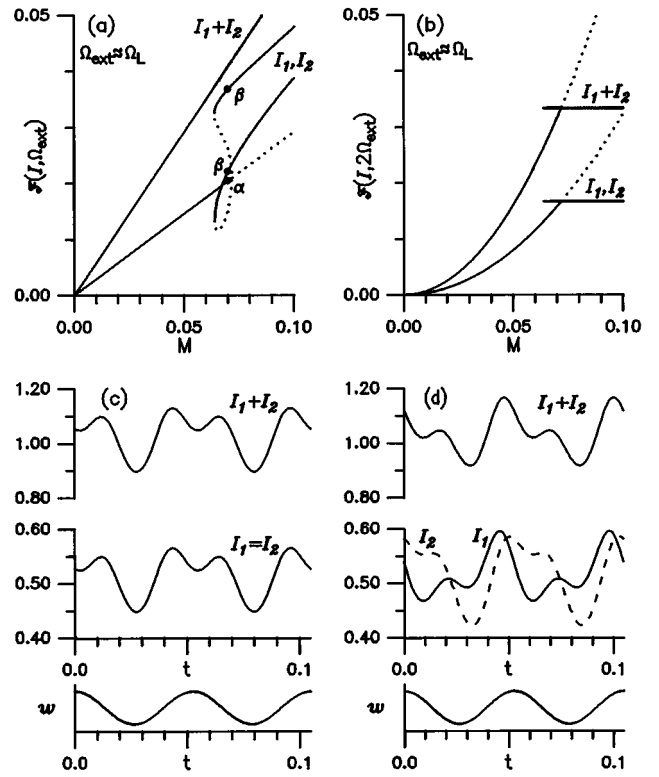


FIG. 5. The detuned symmetric case, with modulation at the low frequency. (a) [resp. (b)]: peak height of the Fourier spectra of I_1 , I_2 and $I_1 + I_2$ at Ω_{ext} (resp. $2\Omega_{\text{ext}}$). The two points α and β , corresponding to $M=0.07$, have been chosen to illustrate the tristable state. For this pump value, two temporal behaviors of the system have been plotted in (c) and (d). I_1 and I_2 are represented by full and dotted lines, respectively, when they are not equal (i.e., when AD is present). (c) corresponds to the $b=0$ solution (point α), while (d) shows one of the two nontrivial solutions (point β). Exchanging I_1 and I_2 gives the third solution. The other parameters are $\kappa=510^4$, $\gamma_2=1$, $w=2.18$, $\Omega_{\text{ext}}=120 \approx \Omega_L$. At the bottom, $w(t)$ has been plotted to give a phase reference. The two points α and β are not reported in (b) for clarity.

into $-b$ if $l_\alpha=0$. Physically, the exchange $b \leftrightarrow -b$ is equivalent to a permutation of the two modes in Eqs. (20). An intriguing feature based on this remark appears when $\Omega_{\text{ext}} \approx \Omega_L$ and $\gamma_2=1$. This is quite clear if b is decomposed into its real and imaginary parts, b_r and b_i , respectively. Inserting this decomposition into the solution (20), the components of $s_{1,1}$ and $s_{2,1}$ at Ω_{ext} defined in (13) are

$$\begin{aligned} s_{1,1}(\Omega_{\text{ext}}) &= 4 \left[\left(\frac{P_1}{12} - b_i \right)^2 + b_r^2 \right]^{1/2} \cos(\tau + \phi_-), \\ s_{2,1}(\Omega_{\text{ext}}) &= 4 \left[\left(\frac{P_1}{12} + b_i \right)^2 + b_r^2 \right]^{1/2} \cos(\tau + \phi_+), \end{aligned} \quad (35)$$

with $\tan(\phi_\pm) = b_r / (P_1/12 \pm b_i)$. Equations (35) demonstrate that the amplitude and the phase of the oscillation at Ω_{ext} are different for the modes s_1 and s_2 : the symmetry between the modes has been spontaneously broken. As a consequence, the bistable state predicted above is in fact a tristable state with $b=0$, $+\sqrt{X_+}$ and $-\sqrt{X_+}$, as illustrated in Fig. 5.

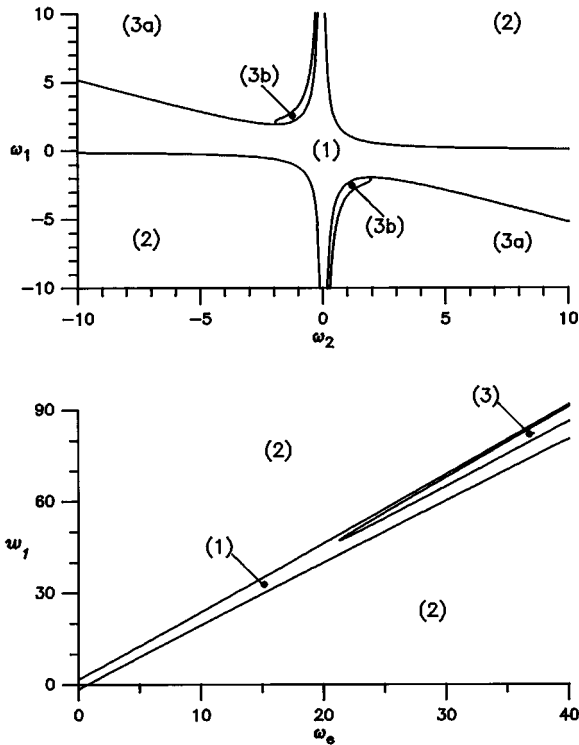


FIG. 6. Parameter planes for $\gamma_2=1$ and/or $\Omega_{\text{ext}} \approx \Omega_R$. In domain (1), there is neither bistability, nor Hopf bifurcation. In domain (2), bistability is found and in domain (3) the stable solution is destabilized by a Hopf bifurcation. Domain 3 has been divided into two parts. In domain 3(a) [resp. 3(b)], a supercritical (resp. subcritical) bifurcation happens, while the separatrix is the locus of vertical bifurcations. Such a division has not been plotted in (b) for clarity. (a) is related to the Eqs. (22) parameters. (b) axes labels are direct physical quantities. Only the first quadrant has been plotted in (b): quadrants 2 and 4 belong to domain (2), and quadrant 3 is symmetric with quadrant 1.

This phenomenon does not exist for $\Omega_{\text{ext}} \approx \Omega_R$ since $P_{\alpha=2}=0$, and the oscillation amplitude is the same for the two modes.

A linear stability analysis around the solutions (31) and (34) shows that $|X_-|$ is always unstable if it exists. $|X_+|$ is stable if $2(75/64 + \omega_1\omega_2) + (75/64)^2 + \omega_2^2 > 0$. Otherwise, it is destabilized by a Hopf bifurcation [28] at $|X_+| = X_H$ with

$$X_H = -\frac{2400}{139^2} \frac{[(\frac{75}{64})^2 + \omega_2^2][(\frac{203}{64})^2 + \omega_2^2]}{2(\frac{75}{64} + \omega_1\omega_2) + (\frac{75}{64})^2 + \omega_2^2}. \quad (36)$$

The condition of destabilization of the solution by the Hopf bifurcation is incompatible with the existence of the bi- or tristable solution. Hence, there are three possibilities, summarized in Fig. 6: a monostable solution (domain 1) without Hopf instability, a bi- or tristable solution without Hopf instability (domain 2), and a monostable solution destabilized by a Hopf bifurcation (domain 3). Domain 3 is subdivided into two parts. In the main part [domain 3(a)], a supercritical Hopf bifurcation leads to the appearance of a new frequency in the solution. This oscillation transforms the periodic solution into a quasiperiodic solution which is stable. In domain 3(b), the Hopf bifurcation is subcritical. Therefore, the quasiperiodic solution emerging from the Hopf bi-

furcation is unstable in the vicinity of the bifurcation point. However this unstable solution becomes stable after a limit point, as in the DOPO case. Thus there is a bistable behavior between a periodic regime and a quasiperiodic regime. The boundary between domain 3(a) and domain 3(b) has been obtained numerically, and corresponds to the locus of existence of a vertical Hopf bifurcation. Note that in all cases, antiphase dynamics persists in the sense that the sum of the oscillating modal intensities is independent of $b(\eta)$, as follow directly from (20).

Eventually, the slightly nonsymmetrical case for which the external modulation Ω_{ext} is close to Ω_L has to be investigated. This requires to consider the full problem Eqs. (22), with $l_\alpha \neq 0$. In the following, the α subscript will not be written anymore since for $\Omega_{\text{ext}} \approx \Omega_L$, α equals 1 by definition. As suggested by the definitions of l and m in Eqs. (23), a new parameter μ is introduced to bind m with l

$$m \equiv \mu l^2, \quad \mu \equiv \left(\frac{8}{9g}\right)^2. \quad (37)$$

Therefore, l becomes the only independent pump parameter and is proportional to the modulation amplitude M . Without loss of generality, we restrict ourselves to $l \geq 0$ since this fixes the phase of the external modulation.

There are two simple particular cases that can be solved analytically. The first of these two cases is the perfectly well tuned asymmetric problem (i.e., $\Omega_L = \Omega_{\text{ext}} = \Omega_R/2, \gamma_2 < 1$) leading to $\omega_1 = \omega_2 = 0$. It can be shown that the steady-state solution $b(l)$ of Eqs. (22) must be real. Taking into account that property, $b(l)$ has to satisfy a third degree polynomial

$$b^3 + b(\frac{75}{64} - \mu l^2) - \frac{75}{64}l = 0. \quad (38)$$

This polynomial has always a real positive solution b_1 . The two other solutions b_2 and b_3 are real only for $l > l_{\text{lim}}$, with

$$l_{\text{lim}} = -\frac{128b_{\text{lim}}^3}{75},$$

$$\begin{aligned} b_{\text{lim}} = & -\left\{ \frac{75}{128^3 \sqrt{\mu}} \left[\left(1 - \sqrt{\frac{\mu-1}{\mu}} \right)^{1/3} \right. \right. \\ & \left. \left. + \left(1 + \sqrt{\frac{\mu-1}{\mu}} \right)^{1/3} \right] \right\}^{1/2} \quad \text{for } \mu \geq 1, \\ = & -\left[\frac{75}{64\sqrt{\mu}} \cos\left(\frac{\arccos(\sqrt{\mu})}{3} \right) \right]^{1/2} \quad \text{for } \mu \leq 1. \end{aligned} \quad (39)$$

If real, b_2 and b_3 are also negative.

The behavior of $b_{1,2,3}$ can be understood by solving Eq. (38) as a second degree polynomial for $l(b)$. The positive solution b_1 equals 0 at $l=0$ and increases with l . Ordering b_2 and b_3 such that $b_1 > 0 > b_2 > b_3$, the solution b_2 is found to increase from $b_{\text{lim}} < 0$ to 0 and b_3 to decrease from b_{lim} to $-b_1(l)$ as l increases from l_{lim} to $+\infty$. Also the point $(l_{\text{lim}}, b_{\text{lim}})$ is a limit point at which b_2 and b_3 join each other.

A linear stability analysis of the solutions $b_{1,2,3}$ provides the following results. Around $l=0$, b_1 is always stable. It is destabilized by a Hopf bifurcation if $\mu < 4096/41209 \approx 0.0994$ at $l=l_h$ with

$$l_h = \frac{1015}{4096} \left[\frac{417}{1 - (\frac{203}{64})^2 \mu} \right]^{1/2}. \quad (40)$$

The solution b_2 is always unstable. If $\mu \leq 4096/5625 \approx 0.7282$, b_3 is unstable. If $0.7282 < \mu \leq 3.4273$, b_3 is stable for $b_3^2 > b_h^2 = 10425/(75^2 \mu - 64^2)$. At $b_3 = b_h$, this solution is destabilized by a Hopf bifurcation. If $\mu > 3.4273$, b_3 is stable over its whole domain of existence $b_3^2 > b_{\text{lim}}^2$.

The second particular case that can be solved analytically requires $g \approx 8/9$. That condition can lead to a remarkable solution for which the oscillation at Ω_{ext} vanishes. If $g = 8/9$, by linking the external frequency $\Omega_{\text{ext}} \approx \Omega_L$ with the pump-modulation amplitude M in such a way that $w_1 = (212/105)\omega_e + 20/21$, ω_1 vanishes and the steady-state solution of system (22) is $a=0$, $b^2=m$. This demonstrates the possibility of canceling the $2\Omega_{\text{ext}}$ component of the solution which then oscillate only at Ω_{ext} . If these conditions on g , w_1 and ω_e are not fulfilled exactly, e.g., if $g = \frac{8}{9} + O(\delta)$ and/or $w_1 = (212/105)\omega_e + 20/21 + O(\delta)$ with $\delta \ll 1$, a small oscillation at $2\Omega_{\text{ext}}$ appears, whose amplitude is $O(\delta)$. A linear stability of this solution shows that it is stable.

We conclude this section by stating that there is a major difference between the symmetric ($\gamma_2=1$) and the asymmetric ($\gamma_2 < 1$) problems in the case of a modulation around Ω_L . In the former problem, there is a bifurcation between the $b=0$ and the $b \neq 0$ solutions. In the later problem, such a bifurcation is absent. By studying the limit $\gamma_2 \rightarrow 1$, it appears that the $b=0$ solution is replaced by a nonzero solution of very small amplitude which is smoothly transformed into an $O(1)$ solution as γ_2 is decreased. This clearly indicates that the bifurcation existing in the symmetric case is not structurally stable.

VI. ANALYTICAL VERSUS NUMERICAL RESULTS

The asymptotic argument $\kappa \gg 1$ has been used to build Eqs. (22). Therefore, it is useful to compare the analytical results with a direct numerical integration of the TSD Eqs. (1). Experimentally, κ can go up to $O(10^6)$ but $\kappa = 5 \times 10^4$ has been chosen because it is a typical value for a yttrium aluminum garnet (YAG) laser. A comparison between the numerical results and the analytical results is shown in Fig. 7. As can be observed, the quantitative validity of our model is very good.

However, two differences have been noticed between the analytical and the numerical results. The first one comes from the existence of a dissymmetry between I_1 and I_2 for the oscillation around Ω_R [Fig. 7(a)]. This dissymmetry is observed numerically if the system is excited at a frequency close to Ω_L and if AD is present, i.e., if $m > m_{\text{thr}}$. But, as the Ω_R oscillation is given for I_1 and I_2 by the same expression in the analytical model [cf. Eqs. (20)], any dissymmetry is absent from the first-order solution. An increase of κ reduces this dissymmetry. Therefore, to catch this feature, the expansion in $1/\sqrt{\kappa}$ should be continued at least an order further.

The second difference concerns the existence and the lo-

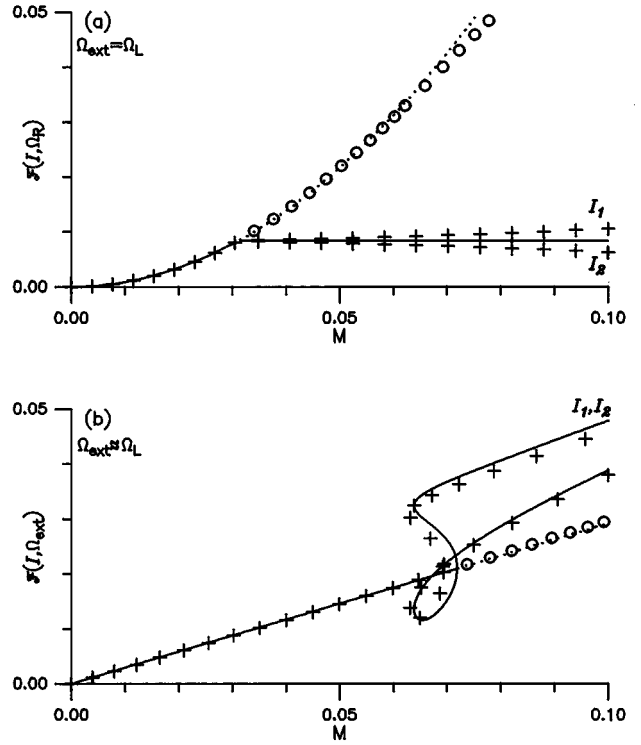


FIG. 7. Analytical vs numerical solutions. (a) [resp. (b)] reproduces Fig. 3(b) [resp. Fig. 5(a)] for I_1 and I_2 with numerical results in addition. The crosses (resp. circles) are the numerical stable (resp. unstable) solutions. The full (resp. dotted) lines are the analytical stable (resp. unstable) solutions.

cation of the Hopf bifurcations. Two mechanisms have been found to destabilize a periodic solution by a Hopf bifurcation. The first mechanism is induced by the detunings ω_1 and ω_2 . In the domain of the Hopf bifurcations, the values required for ω_1 and ω_2 are such that the parameters $|w_1|$ and $|\omega_e|$ have to be, respectively, larger than 47 and 21, for $\gamma_2=1$ [Fig. 6(b)]. This means that for moderate values of κ , the linear approximation used to compute ω_1 and ω_2 may not be precise enough to guarantee that the state of the system stands into the thin zone three of Fig. 6(b). Moreover, the theoretical value of the pump-modulation amplitude at which the model predicts a Hopf bifurcation has to be $O(\epsilon^\alpha)$ to be consistent (with $\alpha=1$ or 2 depending on $\Omega_{\text{ext}} \approx \Omega_L$ or Ω_R , respectively). For example, using $\gamma_2=1$, $\bar{w}=2.615$, $\Omega_{\text{ext}}=289.9$ and $\kappa=5 \times 10^4$, the detunings which are given by Eqs. (23) are $\omega_1=-2.5$ and $\omega_2=1.5$. For these values, the model predicts a Hopf bifurcation at $M \approx 5.53 \times 10^{-3}$. Noting that $M \gg \epsilon^2$, the result is not meaningful and the Hopf bifurcation has not been found numerically. Increasing κ to 5×10^6 and taking $\bar{w}=2.190$, $\Omega_{\text{ext}}=2441.3$ to keep the same value for ω_1 and ω_2 as before, the Hopf bifurcation has been found numerically for a pump modulation only 15% larger than the theoretical predicted value.

The second mechanism leading to a Hopf bifurcation comes from the dissymmetry existing between the two modes of the laser when $\gamma_2 < 1$. For the numerical tests, we chose $\Omega_{\text{ext}} = \Omega_L$ and $w = w_{\text{res}}(\gamma_2)$ in order to have $\omega_1 = \omega_2 = 0$. The other parameters of the two tests we performed were $\gamma_2=0.95$, $\kappa=5 \times 10^4$ and $\gamma_2=0.995$, $\kappa=5 \times 10^6$, respectively, for the first and the second test. For the first set of values, the

numerical pump-modulation amplitude at which the Hopf appears is twice the value predicted by the asymptotic analysis. However, for the second set of parameters, the relative error is reduced to less than 3%.

VII. CONCLUSION

In this paper, an asymptotic model describing a pump-modulated two-mode TSD laser has been derived. This model was aimed at studying the strong energy exchanges existing between the two relaxation frequencies Ω_L and Ω_R when the resonance condition $\Omega_R/\Omega_L \approx 2$ is achieved. As the ratio Ω_R/Ω_L depends on the pump parameter (Fig. 2), the resonance condition is easily fulfilled by adjusting the pumping strength. A weak pump modulation has been used to sustain the intensity oscillations. The main results derive from the analytical study of the model. Pure in-phase and pure antiphased dynamics as well as a mix of antiphase and in-phase dynamics have been predicted and observed numerically. Specifically, it has been shown how antiphase and in-phase dynamics interfere together. We have also charac-

terized secondary bifurcations destabilizing a periodic solution either to another periodic solution (corresponding to a steady-steady bifurcation in the model) or to a quasiperiodic solution (corresponding to a Hopf bifurcation in the model). A multistability domain between two periodic solutions has been found.

In conclusion, our asymptotic analysis succeeded in catching the main properties of the modulated laser. Its qualitative and quantitative validity has been checked via numerical integration.

ACKNOWLEDGMENTS

This research was supported in part by the Interuniversity Attraction Pole program of the Belgian government and by the Fonds National de la Recherche Scientifique (Belgium).

APPENDIX

The inhomogeneous term \vec{N}_2 of the second-order problem is

$$\vec{N}_2 = \begin{pmatrix} -\omega_e[-\frac{7}{4}(s_{1,1}+s_{2,1})+P_\alpha \cos(\alpha\tau)] + \frac{1}{2}(n_{1,1}+n_{2,1}) - 2n_{0,1} \\ [N_{0,1}^0 - \frac{3}{4}(1+\omega_e) - \frac{1}{4}N_{1,1}^0]s_{1,1} + \frac{1}{4}(g - N_{1,1}^0 + \omega_e)s_{2,1} + \frac{1}{4}n_{0,1}^0 - 2n_{1,1} \\ [N_{0,1}^0 - \frac{3}{4}(g+\omega_e) - \frac{1}{4}N_{2,1}^0]s_{2,1} + \frac{1}{4}(1 - N_{2,1}^0 + \omega_e)s_{1,1} + \frac{1}{4}n_{0,1}^0 - 2n_{2,1} \\ -\omega_e(n_{0,1}-n_{1,1}) + (s_{1,1}+I_{1,1}^0-1)(n_{0,1}-n_{1,1}) \\ -\omega_e(n_{0,1}-n_{2,1}) + (s_{2,1}+I_{2,1}^0-g)(n_{0,1}-n_{2,1}) \end{pmatrix}.$$

In this expression, $N_{0,1}^0$, $N_{1,1}^0$, $N_{2,1}^0$, $I_{1,1}^0$, $I_{2,1}^0$ are the first-order terms of the steady-state expansion around the $\epsilon=0$ problem $\gamma_2=1$ and $\bar{w}=w_{\text{res}}(1)=15/7$

$$N_0^0(\bar{w}, \gamma_2) = \frac{8}{7} + \epsilon N_{0,1}^0(w_{1,g}) + O(\epsilon^2),$$

$$N_m^0(\bar{w}, \gamma_2) = \frac{2}{7} + \epsilon N_{m,1}^0(w_{1,g}) + O(\epsilon^2),$$

$$I_m^0(\bar{w}, \gamma_2) = \frac{1}{2} + \epsilon I_{m,1}^0(w_{1,g}) + O(\epsilon^2), \quad m=1,2.$$

Explicitly, they are given by

$$N_{0,1}^0(w_1, g) = \frac{1}{53}(4w_1 + 26g),$$

$$N_{1,1}^0(w_1, g) = \frac{1}{53}(8w_1 + 52g),$$

$$N_{2,1}^0(w_1, g) = \frac{1}{53}(8w_1 - 54g),$$

$$I_{1,1}^0(w_1, g) = \frac{1}{106}(49w_1 + 133g),$$

$$I_{2,1}^0(w_1, g) = \frac{1}{106}(49w_1 - 185g).$$

-
- [1] C. Tang, H. Statz, and G. deMars, *J. Appl. Phys.* **34**, 2289 (1963).
[2] D. McCumber, *Phys. Rev.* **141**, 306 (1966).
[3] K. Otsuka, M. Georgiou, and P. Mandel, *Jpn. J. Appl. Phys.* **31**, L1250 (1992).
[4] K. Otsuka, P. Mandel, S. Bielawski, D. Derozier, and P. Glorieux, *Phys. Rev. A* **46**, 1692 (1992).
[5] P. Mandel, M. Georgiou, K. Otsuka, and D. Pieroux, *Opt. Commun.* **100**, 341 (1993).
[6] K. Otsuka, P. Mandel, M. Georgiou, and C. Etrich, *Jpn. J. Appl. Phys.* **32**, L318 (1993).
[7] D. Pieroux and P. Mandel, *Opt. Commun.* **107**, 245 (1994).
[8] B. Nguyen and P. Mandel, *Opt. Commun.* **112**, 235 (1994).
[9] K. Otsuka, *Phys. Rev. Lett.* **67**, 1090 (1991).
[10] K. Otsuka and J.-L. Chern, *Phys. Rev. A* **45**, 8288 (1992).
[11] K. Wiesenfeld, C. Bracikowski, G. James, and R. Roy, *Phys. Rev. Lett.* **65**, 1749 (1990).
[12] C. Bracikowski and R. Roy, *Phys. Rev. A* **43**, 6455 (1991).
[13] J.-Y. Wang and P. Mandel, *Phys. Rev. A* **48**, 671 (1993).
[14] P. Mandel and J.-Y. Wang, *Opt. Lett.* **19**, 533 (1994).
[15] E. Viktorov, D. Klemer, and M. Karim, *Opt. Commun.* **113**, 441 (1995).
[16] E. Viktorov, O. Orlov, A. Mak, and V. Ustyugov, in *Solid State Lasers*, Vol. No. 1839 of the SPIE Proceedings (SPIE, Bellingham, 1992), p. 337.
[17] T. Erneux and P. Mandel, *Phys. Rev. A* **52**, 4137 (1995).
[18] J.-Y. Wang, P. Mandel, and T. Erneux, *Quantum Semiclass. Opt.* **7**, 169 (1995).

- [19] J.-Y. Wang and P. Mandel, *Phys. Rev. A* **52**, 1474 (1995).
- [20] P. Mandel and J.-Y. Wang, *Phys. Rev. Lett.* **75**, 1923 (1995).
- [21] P. Mandel, K. Otsuka, J.-Y. Wang, and D. Pieroux, *Phys. Rev. Lett.* **76**, 2694 (1996).
- [22] N. Abraham, L. Everett, C. Iwata, and M. Janicki, in *Laser Physics*, No. 2095 in SPIE Proceedings (SPIE, Bellingham, 1993), p. 16.
- [23] J.-Y. Wang and P. Mandel, *Quantum Semiclass. Opt.* **8**, 15 (1996).
- [24] K. McNeil, P. Drummond, and D. Walls, *Opt. Commun.* **27**, 292 (1978).
- [25] P. Drummond, K. McNeil, and D. Walls, *Opt. Acta* **27**, 321 (1980).
- [26] M. Collet and D. Walls, *Phys. Rev. A* **30**, 2887 (1985).
- [27] L. Lugiato, P. Galatola, and L. Narducci, *Opt. Commun.* **76**, 276 (1990).
- [28] N. Pettiaux, R. Li, and P. Mandel, *Opt. Commun.* **72**, 256 (1989).